Anisotropic magnetic properties of $Pr_{1-x}Ca_xMnO_3$

Kenta Okada and Shigeki Yamada

Faculty of Science, Yokohama City University, 22-2 Seto, Kanazawa-ku, Yokohama, Kanagawa 236-0027, Japan

(Received 15 March 2011; revised manuscript received 7 August 2012; published 21 August 2012)

We produced c-axis-oriented samples of $Pr_{1-x}Ca_xMnO_3$ ($0.30 \leqslant x < 0.50$) by applying a uniaxial pressure to quasisingle crystals with multiple domains at a high temperature. This reduced the number of domains in the crystals, allowing better investigation of their anisotropic magnetic properties. Below the Néel temperature, the magnetization curves can be classified into three Ca concentration ranges ($x = 0.3$–0.33, $x = 0.33$–0.37, and $x = 0.4$–0.45). Our results indicate that the magnetic ground state strongly depends on the Ca concentration (x). For $x = 0.30$–0.33, the ground state presents canted antiferromagnetic long-range order, presumably coexisting with ferromagnetic spin clusters. For $x = 0.33$–0.37, the magnetic anisotropy undergoes steep changes near 25 K. These observations suggest the coexistence of ferromagnetic and antiferromagnetic spin clusters. Finally, for $x = 0.4$–0.45, our measurements suggest the presence of small ferromagnetic spin clusters superimposed on the antiferromagnetic long-range order.

DOI: 10.1103/PhysRevB.86.064430 PACS number(s): 75.30.Gw, 75.47.Gk, 75.47.Lx

I. INTRODUCTION

Since the discovery of negative magnetoresistance,[1–6] a family of perovskite manganese oxides $RE_{1-x}AE_xMnO_3$ (where RE is a trivalent rare earth and AE is a divalent alkaline earth element) has attracted considerable attention because the compounds exhibit unusual electrical and magnetic properties. Some of these properties are associated with a charge-ordering state in which Mn^{3+} and Mn^{4+} ions form specific arrangements. This charge ordering occurs in manganese oxides with a small one-electron bandwidth. In $Pr_{1-x}Ca_xMnO_3$, it has been reported that charge-ordering exists for a wide range of x around 0.5 ($0.30 \leqslant x \leqslant 0.75$).[7,8] For $x = 0.5$, Mn^{3+} and Mn^{4+} ions are alternately arranged within the ab plane, with Mn ions of the same valence arranged along the c axis of the $Pbnm$ orthorhombic lattice. For $x < 0.5$, the arrangement of Mn^{3+} and Mn^{4+} ions is the same as for $x = 0.5$, but more than half of the Mn ions are trivalent. Some of the Mn^{3+} ions occupy the Mn^{4+} sublattice. For $x = 0.5$, the Mn spin moments of $Pr_{1-x}Ca_xMnO_3$ are ordered antiferromagnetically due to the superexchange interaction. This is because carrier hopping of e_g electrons of the Mn^{3+} ions is suppressed. On the other hand, for $x < 0.3$, these spin moments are arranged ferromagnetically because of a double exchange interaction. At low temperatures with $0.3 < x < 0.5$, various spin ordering states are expected because of the competition between the double exchange and super-exchange interactions. In fact, there are reports of magnetic phases, e.g., a canted antiferromagnetic phase,[8] a spin glass phase,[9] and phase separation.[10–12] These magnetic phases must be reflected in anisotropic physical properties through symmetries in the charge and spin arrangements. Therefore, measurements of the anisotropic magnetic properties should help clarify the spin ordering states. However, there have been few reports on the measurement of anisotropic properties.[13–15] This is because samples of $Pr_{1-x}Ca_xMnO_3$ have so far been grown by the floating zone method (FZ), and have thus been quasisingle crystals with multiple domains in which pseudo-fourfold axes are mixed. In order to reduce the number of domains and better investigate the anisotropic magnetic properties of the charge ordering phase, we fabricated novel c-axis-oriented samples of $Pr_{1-x}Ca_xMnO_3$ ($0.30 \leqslant x < 0.50$) by applying a uniaxial pressure to quasisingle crystals with multiple domains at a high temperature.

II. EXPERIMENTAL

A series of single crystals of $Pr_{1-x}Ca_xMnO_3$ with $0.30 \leqslant x < 0.50$ was grown by the FZ method. Powders of Pr_6O_{11}, $CaCO_3$, and Mn_3O_4 were mixed, ground, and calcined at 1100°C for 3 h in an air atmosphere and then pulverized. The resultant powder was shaped into cylindrical form at a hydrostatic pressure of 30 MPa to form a feeding and seeding rod. An FZ furnace equipped with two halogen incandescent lamps and hemielliptic focusing mirrors was used for the crystal growth. The molten zone was vertically scanned at a rate of 4 mm/h in an oxygen atmosphere. The powder x-ray-diffraction (XRD) patterns revealed that all samples were single phase. All of the samples were quasisingle crystals with multiple domains in which pseudo-four-fold axes were mixed. $Pr_{1-x}Ca_xMnO_3$ has a cubic lattice structure above 1200°C.[16] We applied a uniaxial pressure of 7 MPa to the quasisingle crystals at 1200°C and cooled them to 1100°C at 1°C per hour (hot press method).[17,18] After hot pressing, an alignment of the c axis parallel to the pressure axis was observed by XRD. The chemical composition was determined by inductively coupled plasma emission spectrometry (Seiko Instruments, Inc. SPS7800). The fluctuation of the Ca composition of all samples was ±0.01. The magnetization was measured using a commercial superconducting quantum interference device magnetometer (Quantum Design Co., Ltd. MPML-XL). The temperature dependence was measured in two distinct processes. In the first, the sample was cooled to 4 K before the first heating run without applying a magnetic field [zero-field cooled (ZFC)]. In the second process, the cooling was done under a magnetic field [field cooled (FC)].

III. RESULTS AND DISCUSSION

Figure 1 shows the temperature dependence of the magnetization for $x = 0.30$–0.45 below 300 K in 1 kOe. As shown in the figure, the magnitude of the magnetization decreased

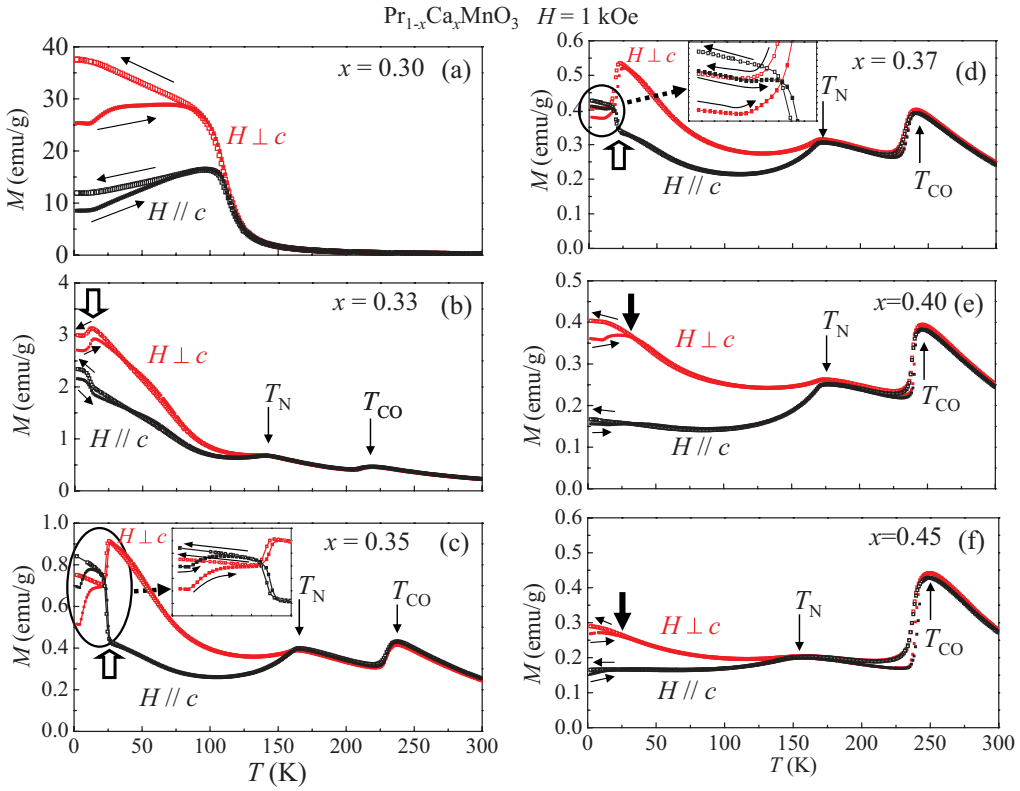

FIG. 1. (Color online) Temperature dependence of the magnetization for $x = 0.33$–0.45 in 1 kOe. The thin solid line arrows indicate the direction of temperature change.

with increasing Ca composition (x). This result is consistent with the magnetic structure changes from antiferromagnetic to ferromagnetic with decreasing x from $x = 0.5$. These magnetization curves can be classified into three Ca concentration ranges ($x = 0.3$–0.33, 0.33–0.37, and 0.4–0.45).

A. The Range of $x = 0.30$–0.33

The magnetization curve of $x = 0.30$ [Fig. 1(a)] has peculiar differences from the other curves. For other x values, the magnetization curves have kinks near 230 K (T_{CO}) and 160 K (T_N), whereas for $x = 0.30$ no such kinks are observable. Near 120 K, magnetization increases rapidly with decreasing temperature, and below this temperature the magnetization in $H \perp c$ is larger than in $H \parallel c$. In this temperature range, the magnetization in FC is different from that in ZFC. To discuss the magnetic ground state of this Ca concentration range, we measured the magnetization curves in a low magnetic field. Figure 2 shows the temperature dependence of the magnetization for (a) $x = 0.30$ and (b) 0.33 in 100 Oe. Figure 2(a) shows the differences between the magnetization in $H \perp c$ and that in $H \parallel c$. This curve increases rapidly with decreasing temperature below 130 K (T_N). The inset of Fig. 2(a) shows the temperature dependence of the inverse magnetic susceptibility ($1/\chi$) for $x = 0.30$. As shown in the inset, the $1/\chi$ plot deviates from a straight line near 210 K (T_{CO}) and has a kink at 110 K (T_{CA}). Below T_{CA}, the magnetization in FC is different from that in ZFC. According to the phase diagram in Ref. 8, T_{CO}, T_N, and T_{CA} are assigned as the charge ordering, antiferromagnetic, and canted antiferromagnetic phase transition temperatures, respectively. For $x = 0.30$, the magnetization curve in 100 Oe is not particularly different from that in 1 kOe except for the anisotropy of the magnetization in ZFC below 70 K. On the other hand, for $x = 0.33$, although the magnetization curve in 1 kOe is comparable to those for $x = 0.35$ and 0.37, the magnetization curve in 100 Oe is comparable to that for $x = 0.30$. This result indicates that there is a phase boundary near $x = 0.33$.

Next, we discuss the magnetic properties in the canted antiferromagnetic phase for $x = 0.30$ in detail. Figure 3 shows the magnetic field dependence of the magnetization at 10 K for $x = 0.30$. At low fields (<15 kOe), the magnetization increases steeply with increasing magnetic field. Between 15 and 35 kOe, an interesting anomalous behavior is observed: a sudden slight change in the slope of the magnetization curves. At higher applied fields (>35 kOe), the magnetization gradually increases with increasing magnetic field. The anomalous behavior between 15 and 35 kOe is observed only under the first increasing field in the first cycle. This behavior corresponds to previous results reported by Tomioka *et al.*[19] These results suggest that the anomalous behavior is caused by a phase transition from canted antiferromagnetic to ferromagnetic. The magnetization curves show isotropic behavior at higher fields and clear anisotropy in a canted antiferromagnetic phase at lower fields. The lower-right inset in Fig. 3 shows an enlarged view of the initial increase and decrease in the magnetic field in the low-field range. In this range, the magnetization in $H \parallel c$ linearly increases with the increasing applied field. On the other hand, the magnetization

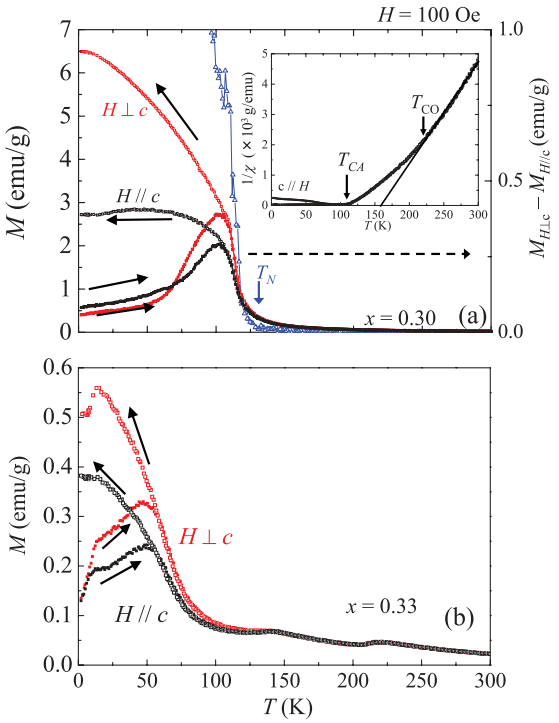

FIG. 2. (Color online) Temperature dependence of the magnetization for $x =$ (a) 0.30 and (b) 0.33 in 100 Oe. The open triangles in (a) represent the difference between magnetization in $H \perp c$ and that in $H \parallel c$. The inset in (a) shows the temperature dependence of the inverse magnetic susceptibility in $H \parallel c$.

curve in $H \perp c$ is not linear. This nonlinearity could be caused by the weak ferromagnetic component perpendicular to the c axis. Below 70K the difference of the magnetic anisotropy between low (100 Oe) and high (1 kOe) applied fields must be due to the difference of this magnetic field dependence of the magnetization. A previous report by Pimenov *et al.*[21] reported the spontaneous magnetization of $La_{0.95}Sr_{0.05}MnO_3$, which has a canted antiferromagnetic long-range ordering, under zero

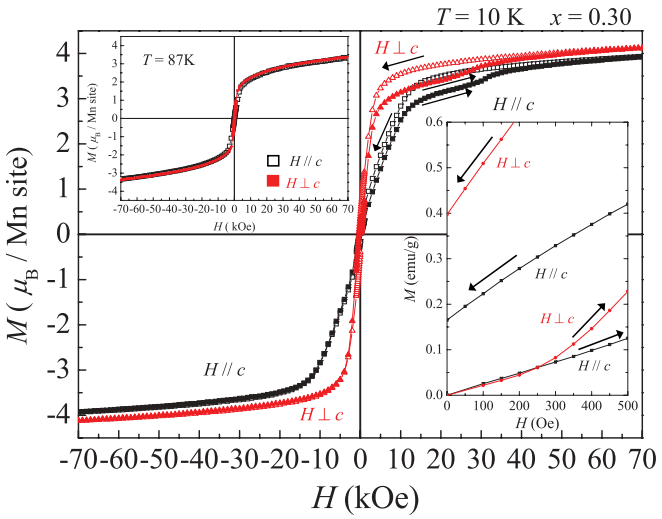

FIG. 3. (Color online) Magnetic field dependence of the magnetization for $x = 0.30$ at 10 K (at 87 K: upper-left inset). The inset to the lower right is a magnified view of the low-field range.

field as a weak ferromagnetic moment. However, as shown in the inset of Fig. 3, the spontaneous magnetizations are not observed for the magnetization of both $H \parallel c$ and $H \perp c$ under an increasing field. This absence of the spontaneous magnetization must be caused by the mixture of the pseudo-fourfold axes in the ab plane and the weak magnetic coercive force of the ferromagnetic phase. In contrast to the magnetization under an increasing field, the magnetizations under decreasing fields have finite values at $H = 0$. This remanence is caused by field-induced reorientation of different magnetic domains of the ferromagnetic component. Therefore, the large difference at 100 Oe between FC and ZFC runs [Fig. 2(a)] can be explained by the reorientation of different domains. Differences in magnetization under FC and ZFC were reported by Deac *et al.*[11] who indicated that the differences were caused by the coexistence of nonmagnetic and magnetic clusters. Sha *et al.*[10] suggested on the basis of neutron diffraction measurements that $Pr_{1-x}Ca_xMnO_3$ ($x = 0.30$) contained ferromagnetic spin clusters in a canted antiferromagnetic ground state. Although our results cannot distinguish the reorientation of the different domain from the ferromagnetic cluster, there are presumably ferromagnetic spin clusters in the canted antiferromagnetic ground state from these previous reports.

A weak magnetic anisotropy is observed, even in the ferromagnetic phase. At 70 kOe, the spin moments are 3.89 ($H \parallel c$) and 4.16 ($H \perp c$) μ_B, which are larger than the full moment of the Mn spins (3.7 μ_B) for $x = 0.30$. This means that Pr spin moments contribute to the magnetization. This contribution could be caused by anisotropy of the ferromagnetic phase; however, this anisotropy is not observed at 87 K (upper-left inset in Fig. 3), which is above the ferromagnetic transition of Pr spins (~60 K)[22]. Since the contribution of Pr ferromagnetic moment was about 0.5 μ_B, the full magnetic moment in the ferromagnetic state is about 4.2 μ_B, larger than that in 70 kOe. However, as mentioned below, for the ferromagnetic phase of other Ca concentration ranges, magnetic anisotropy is not observed. Although this could result from differences in the magnetic structure under a low field, we cannot yet clearly explain these observations solely on the basis of the above magnetization results.

B. The Range of $x = 0.33$–0.37

For this x range [Figs. 1(b), 1(c), and 1(d)], the magnetization curves have kinks near 230 K (T_{CO}) and 160 K (T_N), the charge ordering and Néel temperatures, respectively. No anisotropic magnetic properties are observed near T_{CO}, but a clear anisotropy is observed below the Néel temperature. The magnetization in $H \perp c$ is larger than that in $H \parallel c$. This anisotropy changes near 25 K (open arrow in the figures). At this temperature, the magnetization in $H \perp c$ ($H \parallel c$) steeply decreases (increases). Below this temperature, the magnetization in $H \parallel c$ is larger than that in $H \perp c$, and the magnetization in FC was different from that in ZFC.

Figure 4 shows the magnetic field dependence of magnetization in the antiferromagnetic phase at 50 K for $x =$ 0.35, and the inset shows a magnified view of the low-field range. Although the magnetization in $H \perp c$ is larger than that in $H \parallel c$ below approximately 30 kOe, this magnetic anisotropy vanishes above a kink at 32 kOe (open arrow

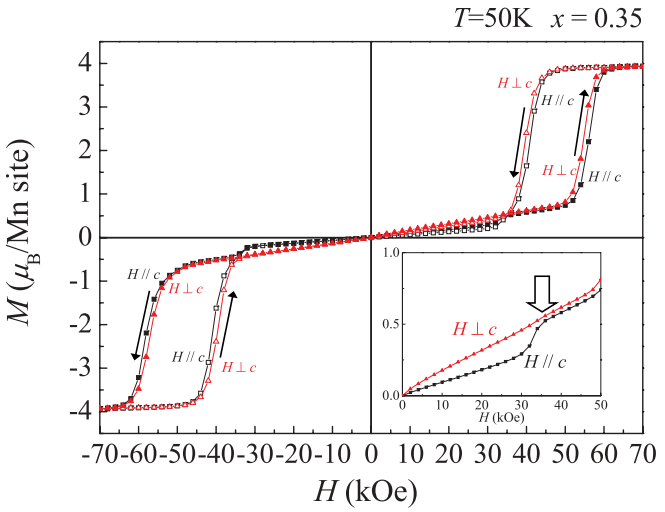

FIG. 4. (Color online) Magnetic field dependence of the magnetization for $x = 0.35$ at 50 K. The inset shows a magnified view of the low-field range.

in the inset). This kink shows that the spins, which are antiferromagnetically arranged along the c axis, flop to the ab plane. This result indicates that the easy magnetization axis of the antiferromagnetic state is the c axis in the low-field range. A metamagnetic transition occurs from the antiferromagnetic state to the ferromagnetically saturated state near 60 kOe. The metamagnetic transition field for $H \perp c$ is slightly smaller than that for $H \parallel c$. However, in the ferromagnetic phase above the metamagnetic transition, no magnetic anisotropies are observed.

Below 25 K, the magnetic anisotropy due to the antiferromagnetic spin order changes, and different magnetization curves are observed for FC and ZFC processes. In measurements under low magnetic fields of about 100 and 10 Oe (Fig. 5), the change of the magnetic anisotropy reflects the magnetic structure at zero magnetic field. These observations correspond to the typical magnetic properties of a spin glass phase. On the other hand, Sha *et al.*[10] reported that the magnetic structure in this temperature range consists of ferromagnetic and antiferromagnetic clusters. In order to investigate the magnetic structure in this temperature range, we measured the magnetic field dependence of magnetization at 18 K (Fig. 6). This magnetization curve has metamagnetic transitions at 50 kOe (in an increasing field) and 10 kOe (in a decreasing field). Above the metamagnetic transition, a ferromagnetic phase is observed. This phase transition corresponds to the phase diagram of Ref. 8. If the magnetic phase in the low-field range at this temperature is that of a spin glass, the magnetization in a decreasing field is larger than that in an increasing field. This effect is called isothermal remanent magnetization.[23] However, below 10 kOe, the magnetization in a decreasing field corresponds to that in an increasing field (see the top-left inset in Fig. 6). This suggests that the magnetic state in this range is not a spin glass phase but consists of coexisting ferromagnetic and antiferromagnetic clusters. In this state, the magnetization has a small anisotropy (the lower-right inset in Fig. 6). In the low magnetic field range, the magnetization in $H \parallel c$ is larger than that in $H \perp c$. However, this anisotropy

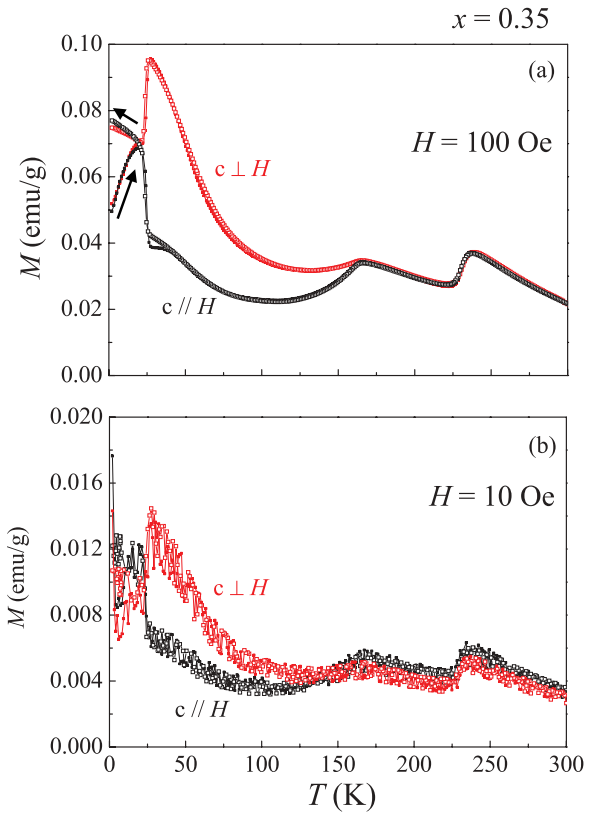

FIG. 5. (Color online) Temperature dependence of the magnetization for $x = 0.35$ in (a) 100 Oe and (b) 10 Oe.

changes at a certain field strength (open arrow in the inset). Above this field, the magnetization in $H \perp c$ is larger than that in $H \parallel c$. Since the ferromagnetic clusters show no magnetic anisotropies in Fig. 6, this magnetic anisotropy must be caused by the antiferromagnetic clusters. The Mn spin moments of $Pr_{1-x}Ca_xMnO_3$ in the antiferromagnetic charge-ordering phase lie in the ab plane for $x = 0.5$ and become directed

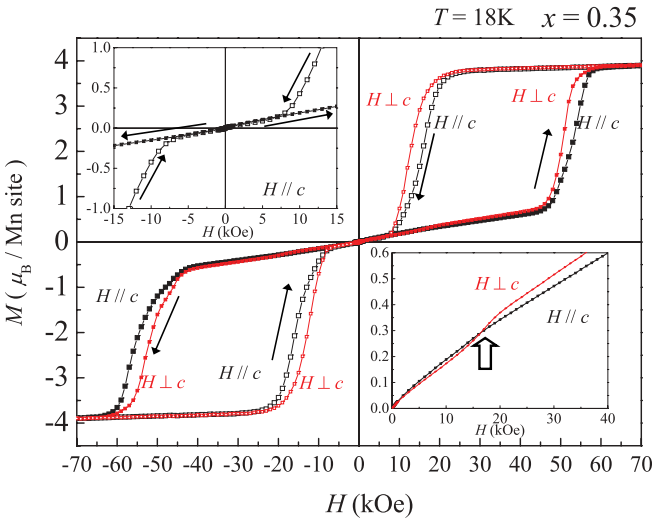

FIG. 6. (Color online) Magnetic field dependence of the magnetization for $x = 0.35$ at 18 K. The upper-left and lower-right insets show the magnetization process dependence and the magnetic anisotropy in the low-field range, respectively.

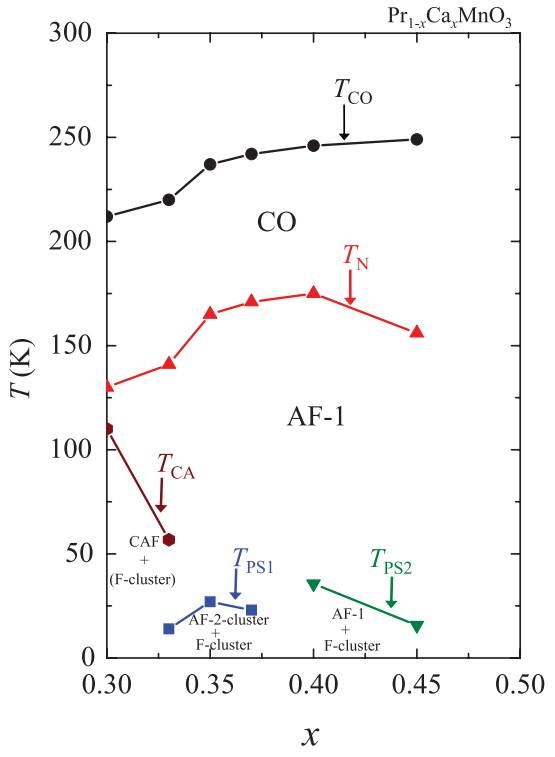

FIG. 7. (Color online) Phase diagram of $Pr_{1-x}Ca_xMnO_3$. CO, AF, and CAF denote the charge order, antiferromagnetic, and canted antiferromagnetic long range order, respectively. The AF labels show the differences in the magnetic anisotropy, i.e., AF-1 and AF-2 are $M_{H\perp c} > M_{H\parallel c}$ and $M_{H\perp c} < M_{H\parallel c}$, respectively. F cluster and AF cluster indicate ferromagnetic and antiferromagnetic clusters, respectively.

toward the c axis with decreasing x from 0.5. For $x < 0.5$, more than half of the Mn ions are trivalent. The e_g electrons of these excess Mn^{3+} ions cause a tilting of the Mn spin moments from the ab plane toward the c axis.[6] Because the arrangement of Mn spin moments in the antiferromagnetic spin clusters corresponds to that for $x = 0.5$, the e_g electrons of any excess Mn^{3+} ions arising from the deviation from $x = 0.5$ are introduced into the ferromagnetic clusters.

C. The Range of $x = 0.40$–0.45

For this x range [Figs. 1(e) and 1(f)], denoted by a bold arrow in the figure, although the magnetization in FC is different from that in ZFC, the magnetic anisotropy does not change. The antiferromagnetic long-range order is maintained for all temperatures below the Néel temperature. Therefore, the differences in magnetization under FC and ZFC could be caused by the small ferromagnetic spin clusters[24] within the antiferromagnetic long range order.

D. Phase Diagram

Figure 7 shows a phase diagram that we have constructed. In this figure, T_{CO} and T_N correspond to the kinks in Fig. 1. For $x = 0.30$, the temperature at which the $1/\chi$ plot deviates from a straight line is T_{CO}, and T_N corresponds to the kink in the temperature dependence of $M_{H\perp c} - M_{H\parallel c}$. For $x = 0.3$–0.33, T_{CA} corresponds to the temperatures at which the magnetization in FC is different from that in ZFC. Below these temperatures, the ground state presents canted antiferromagnetic long-range order, presumably coexisting with ferromagnetic spin clusters. T_{PS1} for $x = 0.33$–0.37 represents the temperatures at which the magnetic anisotropy changes rapidly. Below these temperatures, ferromagnetic and antiferromagnetic clusters coexist. The case of $x = 0.40$–0.45, T_{PS2} corresponds to the temperatures at which the magnetization in FC is different from that in ZFC. Below these temperatures, small ferromagnetic spin clusters are added to the antiferromagnetic long-range ordering.

IV. CONCLUSIONS

We fabricated several c-axis-oriented $Pr_{1-x}Ca_xMnO_3$ crystals under uniaxial pressure and studied their magnetic anisotropy for the first time in the concentration range of $x = 0.30$–0.45. Below the Néel temperature (T_N), the magnetic structure depends on the Ca concentration (x). For $x = 0.33$–0.37, the magnetic anisotropy changes rapidly below 25 K. This result strongly suggests the coexistence of ferromagnetic and antiferromagnetic clusters. In our study, unlike in previous reports,[8] no canted antiferromagnetic phase was observed for $0.35 \leqslant x \leqslant 0.40$.

ACKNOWLEDGMENTS

The authors thank T. Arima and R. Micheletto for useful discussions.

[1] E. K. Chahara, T. Ohno, M. Kasai, and Y. Kozono, Appl. Phys. Lett. **63**, 1990 (1993).
[2] R. von Helmolt, J. Wecker, B. Holzapfel, L. Schultz, and K. Samwer, Phys. Rev. Lett. **71**, 2331 (1993).
[3] Y. Tokura, A. Urushibara, Y. Moritomo, T. Arima, A. Asamitsu, G. Kido, and N. Furukawa, J. Phys. Soc. Jpn. **63**, 3931 (1994).
[4] A. Urushibara, Y. Moritomo, T. Arima, A. Asamitsu, G. Kido, and Y. Tokura, Phys. Rev. B **51**, 14103 (1995).
[5] H. Kuwahara, Y. Moritomo, Y. Tomioka, A. Asamitsu, M. Kasai, R. Kumai, and Y. Tokura, Phys. Rev. B **56**, 9386 (1997).
[6] Y. Tokura and Y. Tomioka, J. Magn. Magn. Mater. **200**, 1 (1999).
[7] Z. Jirak, S. Krupica, Z. Simsa, M. Dlouha, and S. Vratislav, J. Magn. Magn. Mater. **53**, 153 (1985).
[8] Y. Tomioka, A. Asamitsu, H. Kuwahara, Y. Moritomo, and Y. Tokura, Phys. Rev. B **53**, R1689 (1996).
[9] A. Maignan, C. Martin, F. Danny, and B. Raveau, Z. Phys. B **104**, 21 (1997).
[10] H. Sha, F. Ye, P. Dai, J. A. Fernandez-Baca, D. Mesa, J. W. Lynn, Y. Tomioka, Y. Tokura, and J. Zhang, Phys. Rev. B **78**, 052410 (2008).

[11]I. G. Deac, J. F. Mitchell, and P. Schiffer, Phys. Rev. B **63**, 172408 (2001).
[12]P. G. Radaelli, R. M. Ibberson, S.-W. Cheong, and J. F. Mitchell, Physica B **276-278**, 551 (2000).
[13]Y. Okimoto, Y. Tomioka, Y. Onose, Y. Otsuka, and Y. Tokura, Phys. Rev. B **59**, 7401 (1999).
[14]S. Yamada, T. Matsunaga, E. Sugano, H. Sagayama, S. Konno, S. Nishiyama, Y. Watanabe, and T. H. Arima, Phys. Rev. B **75**, 214431 (2007).
[15]S. Yamada, E. Sugano, S. Nishiyama, Y. Watanabe, and T. Arima, J. Magn. Magn. Mater. **310**, 771 (2007).
[16]E. Pollet, S. Krupica, and E. Kuzmicova, J. Phys. Chem. Solids **43**, 1137 (1982).
[17]U. Welp, M. Grimsditch, H. You, W. K. Kwok, M. M. Fang, G. W. Crabtree, and J. Z. Liu, Physica C **161**, 1 (1989).
[18]C. T. Lin, W. Zhon, and W. Y. Liang, Physica C **195**, 291 (1992).
[19]T. Tomioka, A. Asamitsu, Y. Moritomo, and Y. Tokura, J. Phys. Soc. Jpn. **64**, 3626 (1995).
[20]H. Yoshizawa, H. Kawano, Y. Tomioka, and Y. Tokura, Phys. Rev. B **52**, R13145 (1995).
[21]A. Pimenov, M. Biberacher, D. Ivannikov, A. Loidl, V. Yu. Ivanov, A. A. Mukhin and A. M. Balbashov, Phys. Rev. B **62**, 5685 (2000).
[22]D. E. Cox, P. G. Radaelli, M. Marezio and S-W. Cheong, Phys. Rev. B **57**, 3305 (1998).
[23]J. A. Mydosh, *Spin Glasses: An Experimental Introduction* (Taylor & Francis, London, 1993).
[24]N. Biškup, A. de Andrés, and M. Garcia- Hernández, Phys. Rev. B **78**, 184435 (2008).